ISSN 1392-1207. MECHANIKA. Vol. 32, No. 2, 2026: 100–106

Simulation on the Impact of Porosity on the Properties of Ceramic Particles Reinforced Metal Matrix Composites

Khelifa MANSOURI*, Hamid DJEBAILI, Faicel KHADRAOUI***, Mourad CHITOUR****, Abdelhak BERKIA*****, Sofiane TOUATI******, Farid LEKMINE*******, Dalel BOURMADA********

**Abbes LAGHROUR University, Khenchela, 40000, Algeria, E-mail: mansouri.khelifa@univ-khenchela.dz*
***Abbes LAGHROUR University, Khenchela, 40000, Algeria, E-mail: djebaili_hamid@univ-khenchela.dz*
****Abbes LAGHROUR University, Khenchela, 40000, Algeria, E-mail: faicel.khadraoui@univ-khenchela.dz*
*****Abbes LAGHROUR University, Khenchela, 40000, Algeria, E-mail: chitour.mourad@univ-khenchela.dz*
******Abbes LAGHROUR University, Khenchela, 40000, Algeria, E-mail: berkia.abdelhak@univ-khenchela.dz*
*******Abbes LAGHROUR University, Khenchela, 40000, Algeria, E-mail: sofiane.touati@univ-khenchela.dz*
********Abbes LAGHROUR University, Khenchela, 40000, Algeria, E-mail: farid.lekmine@univ-khenchela.dz*
*********Abbes LAGHROUR University, Khenchela, 40000, Algeria, E-mail: bourmada.dalel@univ-khenchela.dz*

https://doi.org/10.5755/j02.mech.42248

1. Introduction

Composite materials are defined as polyphase materials that consist of multiple non-single component substances combined through composite processes. Compared to traditional materials, composite materials and structures are characterized by their designability, identity, and reliance on composite technology [1]. Metal matrix composites that are reinforced with particles exhibit significantly superior stiffness and strength relative to the matrix alloys, resulting in their prevalent use in the automotive industry, as well as in aircraft and aerospace constructions [2]. Recently, silicon-carbide-reinforced composites have attracted considerable interest due to their exceptional properties, including high strength, thermal conductivity, and electrical conductivity [3].

Porosity, as a critical microstructural attribute of particle-reinforced composites, significantly impacts the mechanical, thermal, and electrical properties of these materials. As porosity is an unavoidable occurrence during the manufacturing of silicon-carbide-reinforced composites, it is vital to explore the influence of porosity on the properties of the material to enhance its overall performance [3].

Furthermore, various scholars have explored the mechanical properties of particle-reinforced composites. According to J.L. Christian et al. [4], the primary cause of porosity formation lies in the casting parameters, these parameters include the casting route employed, the stirring speed and position of the impeller, the volume fraction of the reinforcement material, and the process parameters, which consist of the holding time [5]. Dipti Kanta Das et al. [6], noted that the tensile and flexural strength improved up to a specific reinforcement fraction in the composites, after which these strengths diminished. The initiation and propagation of fine microcracks ultimately result in macroscopic failure. Yiwu YAN et al. [2], employed the finite element method to explore how particle size influences the deformation characteristics of SiCp/Al composites. It has been established that the flow stress and work hardening rate of the composite rise as the particle size diminishes, while maintaining a constant volume fraction of the reinforcement. Parvez Alam [7] established a model for mixtures that accurately estimates the Young modulus of porous particle–polymer composites. The model was assessed in relation to classical mixtures models and more recent porous composite models by comparing it to computational simulations and experimental outcomes. Mengqin Chen [8] and colleagues conducted research on SiC/Al composites characterized by a high volume fraction of SiC particles. They examined the impact of particle size on the porosity of the preform. Furthermore, the preform was infiltrated with various Al alloys, and the correlation between porosity and thermal conductivity of SiC/Al was investigated. Xiaohong Xu et al. [9], established that a reduction in the size of SiC particles not only substantially increases the bending strength of porous SiC membrane supports but also slightly decreases the firing temperature, attributed to the smaller SiC particles having a higher specific surface area and greater reactivity. K. Mansouri et al. [10], investigate the role of porosity in determining the mechanical properties of Aluminum matrix composites that are reinforced with ceramic particles, with a focus on optimizing volume fraction and porosity to enhance tensile strength, the results showed that as porosity increased, there was a corresponding increase in Von Mises stress, while higher volume fractions contributed to improved stress distribution and enhanced mechanical properties. The research conducted by Yicheng Jin et al. [11], focused on the impact of preform pore size on the mechanical properties and thermal expansion coefficients of the composites. As a result, a further decrease in the size of the preform pores could lead to a decline in the mechanical and thermal properties of the composites. Tao Zeng [12] and his team investigated the fabrication of SiC reinforced Aluminum composite foams through laser melting deposition. They found that as the concentration of SiC nanoparticles increased, both the porosity and the average pore size of the aluminum foams diminished. Jorge E. and Rivera-Salinas [13] investigates the influence of porosity on the Young's modulus of SiC reinforced aluminum matrix composites, they determined that the elastic properties of the composite are particularly affected by pores located away from the reinforcement. It has been established that the reduction in the elastic modulus is attributable to the existence of pores. M. Kupkova and L. Parilak [14], in their publication, provided calculations for the Young modulus of samples featuring periodically distributed spheroidal pores, along with the

relationship of this modulus to overall porosity, pore size, orientation, and anisotropy. Their findings indicate that the presence of pores that are flattened in the direction of loading significantly diminishes the Young's modulus value, even at low levels of porosity. In her analysis, Barbara Silver-Thorn [15] outlines the progression and formulation of relationships relevant to the effective Young's modulus of porous materials, ultimately concluding that verifiable equations that yield consistently reproducible results associated with specific pore structures are not yet available. Zhigao Chen et al. [16], show that the SiCp/Al composite material has different material properties due to variations in the volume fraction of SiC particles. The specific performance characteristics of aluminum matrix composite materials indicate that an increase in volume fraction results in a higher composite Young modulus. M. Montoya-Dávila et al. [17], examine the influence of the particle size distribution of SiC particulate reinforcements on the Young's modulus of composites produced through reactive infiltration. The findings indicate that as the particle size distribution increases, the residual porosity diminishes, leading to enhancements in both the density and Young's modulus of the composites. The tensile strength and yield strength values reported by Venkata Surya Dinesh C. [18] reveal that the ultimate tensile strength rises with an increase in Al_2O_3 content, while the yield strength decreases as the reinforcement particle size increases. The ultimate tensile strength continues to rise.

This research seeks to explore how porosity affects the performance of SiC reinforced aluminum matrix composites that exhibit porosity. To accomplish this, we examine both constant pore diameters, presuming a circular configuration while keeping the volume fraction constant. The secondary aim is to calculate the Young's modulus of the composite using finite element analysis and to compare the outcomes with other theoretical models.

2. Homogenization Models

The Young's modulus of a particle-reinforced composite can be estimated using several empirical and theoretical approaches. The porosity of the material is an important factor to consider, as it can reduce the stiffness and strength of the composite.

2.1. Dewey model

Dewey [19] derived expressions for the elastic constants of materials with non-rigid fillers in the dilute limit by considering a single sphere (radius = R) within an isotropic medium that is subjected to a displacement at a large distance ($\gg R$) from the sphere. Thus, these expressions are applicable to 'very dilute suspensions' where surface effects can be ignored:

$$E_c = E_0 \times (1 - aP). \tag{1}$$

In this context, E_c represents Young's modulus of the porous composite, while E_0 denotes the modulus of a non-porous variant of the same composite. The constant 'a' is influenced by the Poisson's ratio of the matrix material, and 'P' indicates the porosity fraction (with values ranging from 0, indicating no pores, to 1, indicating complete porosity).

2.2. Paul model

According to Paul [20], the most basic relationship between material properties and porosity that adheres to the boundary conditions is the "rule of mixtures" for two-phase solids. This principle is founded on the assumption that both materials contribute to the composite's stiffness in proportion to their individual moduli and fractional volumes (particular case of the Dewey equation):

$$E_c = E_0 (1 - P). \tag{2}$$

2.3. Voigt model

The Voigt model (stress approach) [21] is often used to estimate the mechanical properties of composites. For the Young's modulus E_c of a composite with particles, a classic approach is to use the rule of mixtures:

$$E_c = V_p E_p + V_m E_m. \tag{3}$$

Here:

- V_m and V_p are the volume fractions of the matrix and the reinforcing particles, respectively;
- E_m and E_p are the Young's modulus of the matrix and the particles, respectively.

A common approach to account for porosity is to modify the volume fractions of the components by integrating porosity into the calculation:

$$E_c = V_p E_p + V_m E_m \times (1 - P). \tag{4}$$

2.4. Reuss model

The Reuss model (strain approach) [22] can also be used to estimate Young's modulus:

$$\frac{1}{E_c} = \left(\frac{V_p}{E_p} + \frac{V_m}{E_m} \right), \tag{5}$$

where E_c represents the modulus of the zero porosity material and can be determined by extrapolation. By integrating porosity into the calculation, and use of the Reuss equation becomes the McAdam model [23]:

$$\frac{1}{E_c} = \left(\frac{V_p}{E_p} + \frac{V_m}{E_m} \right) \times (1 - P). \tag{6}$$

2.5. Halpin-Tsai model

Shuiwen Zhu et al. [24], introduces an improved Halpin–Tsai model to predict the mechanical properties of SiC reinforced polypropylene composites. The model considers the influence of porosity and corresponding silicon-carbide volume fractions and derives relationships between material property shape factors and the aspect ratio:

$$E_c = E_m \frac{1 + \xi_e \eta V_p}{1 - \eta V_p}, \tag{7}$$

with $\eta = \left(E_p/E_m - 1\right)/\left(E_p/E_m + \xi\right)$ and $\xi_e = a + b \times P + 2c \times \alpha \times V_p$, where ξ_e is the modified mechanical shape factor; a, b, and c are fitted constant values. $\alpha = l/2R$ is the aspect ratio of the reinforcing phase and R and l are the radius and length of particles, respectively. The matrix porosity was assumed circular and random distribution of pores ($\alpha = 1$). Through the improved Halpin–Tsai model, the relationship between the shape factor and porosity is obtained:

$$\xi_e = 1.07042 - 21.2374 \times P + 4.3682 \times V_p . \quad (8)$$

3. Numerical Simulation

Finite Element Analysis (FEA) has established itself as a commonly adopted method for representing the mechanical behavior of metal matrix composites, especially those that consist of aluminum and silicon carbide (SiC). This study examines how the volume fraction of SiC particles and the distribution of pores affect the Young's modulus in aluminum matrix composites. Considering the model's limited scale, a refined mesh consisting of triangular elements was implemented (Fig. 1) [25].

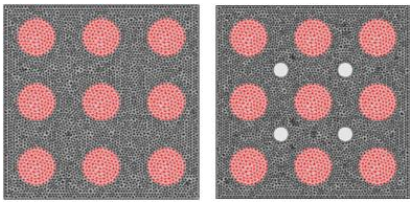

Fig. 1 Composite mesh with triangular elements for composite without and with voids

The model operates under the assumption that the SiC particles are completely bonded to the matrix, thus preventing any interfacial slip or debonding from happening between the particles and the matrix material. This assumption is crucial for effectively modeling the perfect interaction between the reinforcing particles and the matrix [26]. Each component of the composite is presumed to exhibit isotropic characteristics: All particles possess the same diameter (d_p), the specimen is represented as a two-dimensional elastic entity, the configuration of particles and pores is regularly repeated throughout the composite and pores are of circular shape, which facilitates calculations and comparisons.

3.1. Composite properties

The matrix is presumed to possess a square configuration with a side length of l_m = 155.425 μm, and simulations were performed utilizing CASTEM finite element software [27]. Composites comprising nine SiC particles (N_p = 9) were represented in three distinct packing configurations: square, hexagonal, and random. For the objectives of this research, the composite is designed to include four circular pores (N_v = 4) (illustrated in Fig. 2 and Fig. 3).
The following parameters are applied in all computational processes:
1. SiC particles: Young's modulus E_p = 485 GPa, Poisson ratio ν_p = 0.2, and density ρ_p = 3.2 g/cc [28].

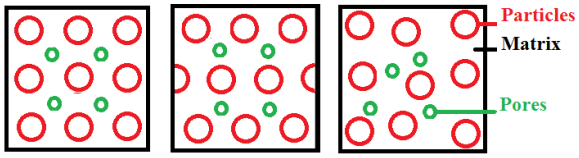

Fig. 2 Composites with four pores of same diameter

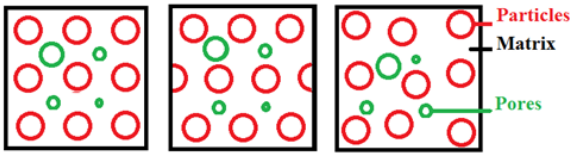

Fig. 3 Composites with four pores of different diameter

2. Aluminium matrix: Young's modulus E_m = 70 GPa, Poisson ratio ν_m = 0.33, and density ρ_p = 2.7 g/cc [29].

3.2. Geometric parameters

Composite volume can be expressed by Eqs. (9), (10) where V_p is the particle volume fraction, V_m is the matrix volume fraction and V_v is the void volume fraction. Eq. (9) describes the ideal composite volume fraction and Eq. (10) describes the true volume fraction.

$$V_p + V_m = 1 , \quad (9)$$

$$V_p + V_m + V_v = 1 . \quad (10)$$

In theory, the theoretical density should consist exclusively of particles and resin, without any void inclusions. Voids increase the volume but do not contribute to mass, leading to a decrease in density. Therefore, the variation between the theoretical density and the measured density of the composite represents the porosity in terms of volume fraction. In the theoretical analysis, particles are modeled to be uniformly packed in regular arrangements.

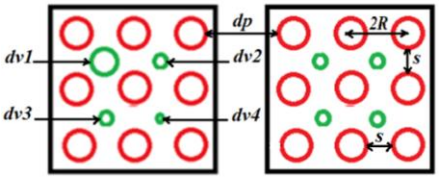

Fig. 4 Composite data

The particle volume fraction (V_p) of these ideal arrangements can be computed as:

$$V_f = \frac{V_{particle}}{V_{total}} = \frac{N_p\left(\pi d_p^2/4\right)}{l_m l_m} \Rightarrow d_p = \sqrt{\frac{4V_f l_m^2}{N_p \pi}} , \quad (11)$$

where $2R$ is the center to center spacing of nearest neighbor particles.

Eq. (12) gives the expression for the separation of particles (s) into ideal arrangements (Fig. 4):

$$s = \frac{\left(l_m - \left(3 \times d_p\right)\right)}{3} . \quad (12)$$

These ideal packing arrays are generally used to develop micromechanical models due to their simplicity. However, they are not observed in real composites except in a few localized regions. The diameters d_p and distance s calculate using Eqs. (11) and (12) are summarized in Table.1.

Table 1
Particles diameter as a function of volume fraction

V_f	0.05	0.10	0.15	0.20	0.25	0.30	0.35
d_P, μm	16.82	23.79	29.14	33.65	37.62	41.21	44.41
s, μm	49.87	42.87	37.52	33.01	29.04	25.45	22.15

3.3. Voids diameter

From Eq. (11), we can deduce the diameter of the voids d_{Void} using the same reasoning as for the particles.

$$d_{Void} = \sqrt{\frac{4V_{fVoid}l_m^2}{N_{Void}\pi}}, \tag{13}$$

where: V_{fVoid} is voids volume fraction; N_{Void} is a number of voids. Table 2 summarizes the results of the diameter calculations.

Table 2
Voids diameter as a function of porosity

V_f	0.01	0.02	0.03	0.04	0.05
d_{Void}, μm	11.28	15.96	19.54	22.57	25.23

In the case of voids with diameter not constant (Fig.4), we have supposed that the relation between voids diameters is:

$$2d_{Voids1} = d_{Voids2} = d_{Voids3} = \tfrac{1}{2}d_{Voids4} = d_{Voids}, \tag{14}$$

3.4. Boundary conditions

The preferred method is the application of periodic boundary conditions, the use of periodicity is crucial because uniform boundary conditions artificially "lock" the material (edge effect). Block UY on the right side and leave UX free. At the other side, we applied a tensile stress of $\sigma_x = 5.65\times10^{-8}$ N/μm^2, that is, for $x = 0$ and $x = l_m$ [30].

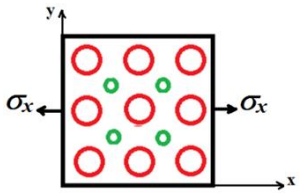

Fig. 5 Boundary conditions for square package

4. Results and Discussion of the Numerical Simulation

The numerical data were contrasted with the predictions generated by multiple theoretical models, including the Voigt and Reuss models, the improved Halpin–Tsai rule, and the FEA (SiC/Al composite).

4.1. Von Mises stresses distribution

Fig. 6 depicts the distribution of Von Mises stresses in a composite material characterized by a particle volume fraction. The simulation performed indicates that high concentrations of stresses are present in the SiC particles and in the matrix area situated between these particles. The presence of voids leads to discontinuities in the stress distribution; this is attributed to the formation of a plastic zone in this region, which may result in fractures occurring in the matrix area between the reinforcements. Furthermore, it is noteworthy to mention the zones of stress concentration that appear around the voids.

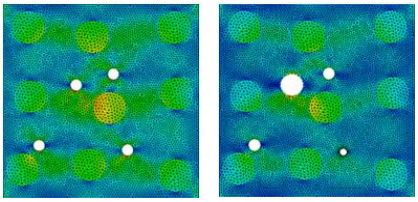

Fig. 6 Von Mises stresses distribution for $V_p = 20\%$ and $V_{fVoids} = 1\%$ (random package)

4.2. Porosity effect

We investigate in this section the composite material with circular pores of the same radius. The stress distributions of Von Mises in the composites, which lack defects and pores across the three packing, are depicted in Fig. 7. It can be noted that the Von Mises stresses decrease with an increase in the volume fraction of the SiC reinforcement across all three packing, stabilizing at a volume fraction of 20%. In contrast, the random arrangement, which is a more accurate representation of real composites, shows the highest stress value. This is attributed to the closer proximity of particles in random arrangements, which leads to localized concentrations of additional stresses.

Within the composite characterized by porosity, it is

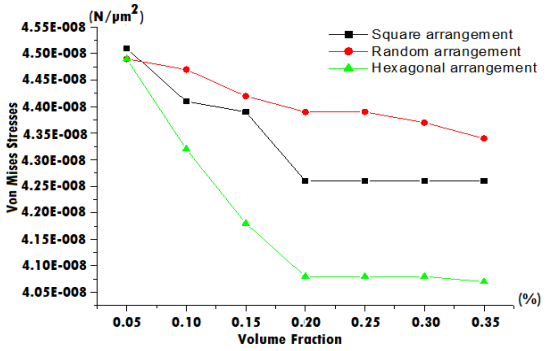

Fig. 7 Evolution of Von Mises stresses in function of volume fraction (no pores)

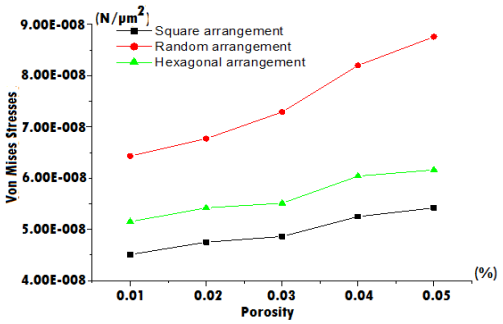

Fig. 8 Evolution of Von Mises stresses in function of porosity ($V_p = 20\%$)

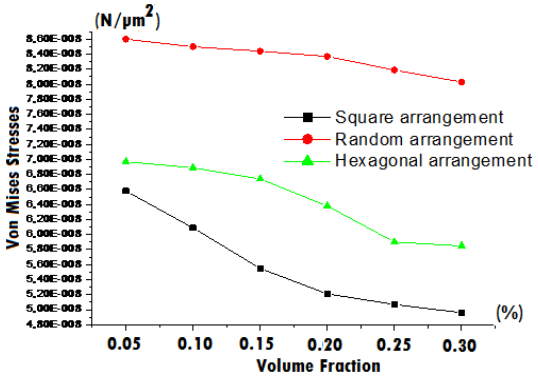

Fig. 9 Evolution of Von Mises stresses in function of volume fraction (V_{voids} = 4%) for d_{voids} constant

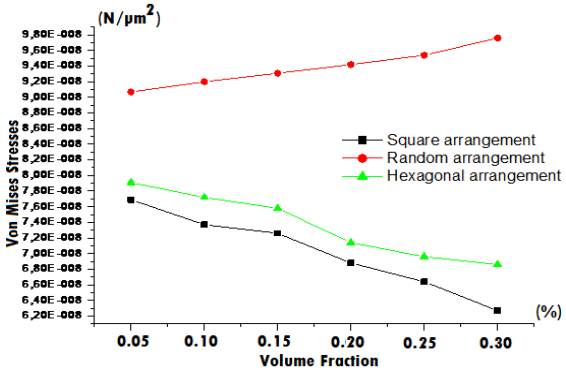

Fig. 10 Evolution of Von Mises stresses in function of volume fraction (V_{voids} = 4%) for d_{voids} variable

noted that an increase in porosity leads to a corresponding increase in stresses (Fig. 8). The random distribution indicates that the stress values are markedly greater in comparison to the square and hexagonal arrangements; this can be explained by the presence of pores among the particles, which in turn intensifies the stress concentrations.

Fig. 9 and Fig. 10 represent the evolution of Von Mises stresses on particles volume fraction where the porosity is taken V_{Voids} = 4%. As volume fraction increase from 0.05 to 0.25%, the particles become relatively smaller compared to the voids due to the fixed voids volume fraction. As a result, the Von Mises stress decreases for the three arrangements. Note that in Fig. 10 and for the random package, the stresses increase because voids get closer to the particles, consequently the matrix is less present in interparticles which facilitates the propagation of cracks between these particles.

4.3. Young's modulus

The modeling of the interaction between particles and the matrix, or the interaction between pores and the matrix at the microscale, is beneficial for accurately predicting effective properties such as Young's modulus.

In Fig. 11, the bounds on Young's modulus for the Al/SiC composite are compared, drawing from numerical data generated in this study. The results demonstrate that Young's modulus tends to evolve in a nearly linear fashion with respect to the volume fraction; it is observed that the Young's modulus values in the random arrangement are much greater than those found in the square arrangement.

Fig. 12 shows the development of Young's modulus as a function of porosity for the square layout, with reinforcement volume fractions between 5% and 30%. It is evident that Young's modulus declines with increasing porosity and conversely rises with an increase in volume fraction.

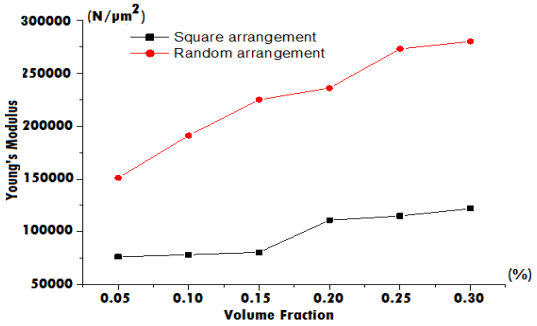

Fig. 11 Effect of reinforcement content on the elastic modulus of Al/SiC composite without pores

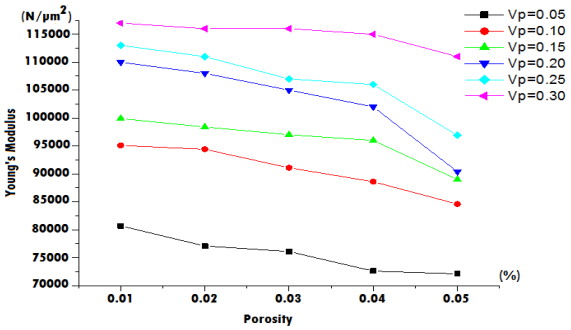

Fig. 12 Effect of porosity on the elastic modulus of Al/SiC composite for square arrangement

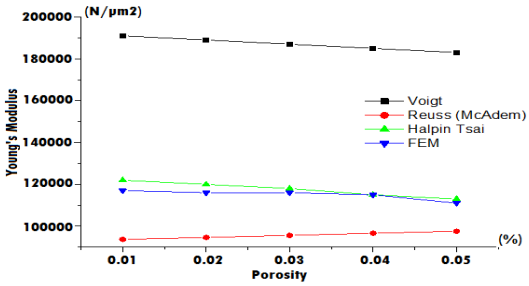

Fig. 13 Evolution of porosity on the elastic modulus of Al/SiC composite

The effective Young's modulus comparisons predicted by finite element and analytical micromechanics models are shown in Fig. 13. In the analyzed cases that consider the coexistence of pores within the matrix, the most significant impairment of the Young's modulus of the composite was found in the scenario of a fully dense particle and a porous matrix. Among these models, those proposed by Voigt and Reuss have proven to be effective approaches for establishing upper and lower bounds for the elastic modulus of the composite based on the known properties of its constituents. We also note in the figure that the results obtained by FEM are in good agreement with those of Halpin-Tsai.

An augmentation of the reinforcement volume fraction indicates a corresponding increase in the content of silicon carbide, which is associated with a higher elastic modulus. The incorporation of silicon carbide particles can significantly enhance the stiffness and strength of composite materials, thereby increasing the elastic modulus.

Therefore, within a particular range, an increase in the SiC volume fraction enhances the rigidity characteristics of the material, leading to an increase in the elastic modulus.

At this point, any further increase in the volume fraction may lead to a decline in other performance characteristics.

The porosity in MMCp arises from various origins, which makes it important to analyze the inhomogeneous stress field around pores that interact with hard particles, as well as the negative effect that the discontinuity caused by these pores has on the load-bearing capacity of the MMCp. Despite the presence of pores in the composite, the transfer of stress from the soft matrix to the hard particle is effective in all cases, the rationale behind this is that an increase in porosity introduces more voids and holes within the material, which disrupts its continuity and integrity, leading to a reduction in load transfer efficiency and an increase in material deformation. Pores and holes hinder the uniform distribution of stress in the material, which results in greater material deformation and a subsequent decrease in the elastic modulus.

5. Conclusions

The FEM analysis facilitates the forecasting of the properties of aluminum matrix composites reinforced with SiC particles, while also addressing the impact of porosity by incorporating additional variables such as the size of the particles, their distribution, and the effects of their interactions. The data demonstrates that the composite's properties are particularly responsive to the porosity within the matrix, due to the greater stiffness of the particles relative to the matrix. It has been observed that the stress levels are higher in the model characterized by pores of different sizes compared to those with a uniform diameter. This phenomenon can be explained by the increase in void size, which amplifies the matrix's discontinuity, resulting in a significant concentration of stress.

The research findings indicate that an increase in porosity correlates with a decrease in Young's modulus. Conversely, a higher volume fraction of particle reinforcement is associated with an increase in the elastic modulus of the composite material. This suggests that materials with greater porosity are more flexible and less resistant to deformation than those with lower porosity. Pores serve as defects, which reduce the contact area between the phases of the composite, thereby decreasing its ability to withstand stress. The presence of pores can lead to a reduction in the stiffness of the composite, making it more flexible and less capable of resisting deformation. Additionally, porosity can create channels for crack propagation and facilitate the degradation of the composite due to moisture, chemicals, or loading cycles.

In the analysis of finite-element simulated values against the predictions made by the improved Halpin–Tsai model, it becomes clear that the finite-element method (FEM) shows remarkable precision in assessing the performance of aluminum composites that are reinforced with silicon-carbide particles. Thus, FEM is a trustworthy technique for predicting the performance of such composite materials, concurrently facilitating the simplification of performance parameter calculations.

References

1. **Lu, M.Y.; Han, B.H.; He, W.H.; Cheng, Z.G.; Yu, J.F.** 2021. The strength of the ceramic matrix composites under the influence of pore is reviewed, The 9th Global Conference on Materials Science and Engineering (CMSE 2020) Journal of Physics: Conference Series 1777: 012027. https://doi.org/10.1088/1742-6596/1777/1/012027.
2. **Yan, Y.W.; Geng, L.; Li, A.B.; Fan, G.H.** 2007. Finite Element Analysis about Effects of Particle Size on Deformation Behavior of Particle Reinforced Metal Matrix Composites, Key Engineering Materials 353-358: 1263-1266. https://doi.org/10.4028/www.scientific.net/KEM.353-358.1263.
3. **Mao, D.; Meng, X.; Xie, Y.; Yang, Y.; Xu, Y. ; Qin, Z.; Chang, Y.; Wan, L.; Huang, Y.** 2022. Strength-ductility balance strategy in SiC reinforced aluminum matrix composites via deformation-driven metallurgy, Journal of Alloys and Compounds 891: 162078. https://doi.org/10.1016/j.jallcom.2021.162078.
4. **Christian, J.L.; Forest, J.D.; Weisinger, M.D.** 1970. Aluminum-Boron composites for aerospace structures, Ft. Belvoir Defense Technical Information Center. USA.
5. **Priyadarshi, D.; Sharma, R.K.** 2016. Porosity in aluminium matrix composites: cause, effect and defence, Materials Science: An Indian Journal 14(4): 119-129.
6. **Das, D.K.; Mishra, P.C.; Singh, S.; Thakur, R.K.** 2014. Properties of ceramic-reinforced aluminium matrix composites - a review, International Journal of Mechanical and Materials Engineering 9: 12. https://doi.org/10.1186/s40712-014-0012-9.
7. **Alam, P.** 2010. A mixtures' model for porous particle–polymer composites, Mechanics Research Communications 37(4): 389-393. https://doi.org/10.1016/j.mechrescom.2010.04.002.
8. **Chen, M.; Bai, Y.; Zhang, Z.; Zhao, H.** 2021. The Preparation of High-Volume Fraction SiC/Al Composites with High Thermal Conductivity by Vacuum Pressure Infiltration, Crystals 11(5): 515. https://doi.org/10.3390/CRYST11050515.
9. **Xu, X.; Liu, X.; Wua, J.; Ma, S.; Liu, S.; Chen, T.** 2022. Effect of SiC Particle Size on Properties of SiC Porous Ceramics, Journal of Wuhan University of Technology-Materials Science Edition 37: 13-22. https://doi.org/10.1007/s11595-022-2493-3.
10. **Mansouri, K.; Touati, S.; Boumediri, H.; Djebaili, H.; Chitour, M.; Zemmouri, A.; Khadraoui, F. ; Berkia, A.** 2025. Numerical Modeling and Optimization of Mechanical Properties in Porous Aluminum Matrix Composites Reinforced with SiC Particles, Materials Research 28: e20240474. https://doi.org/10.1590/1980-5373-MR-2024-0474.
11. **Jin, Y.; Zhang, B.; Liu, Q.; Zhong, Z.; Zhang, H.; Ye, F.; Zhang, Z.** 2021. Fabrication of co-continuous SiC/Al composites from novel SiC preforms with high porosity and controllable pore size, Ceramics International 47(2): 2766-277. https://doi.org/10.1016/j.ceramint.2020.09.130.
12. **Zeng, T.; Liu, Y.; Wang, L.; Gao, Y.; Wang, R.** 2022. Fabrication of Al/SiC composite foams with TiH_2 foaming agent by laser melting deposition, Materials Research Express 9(4): 046514. https://doi.org/10.1088/2053-1591/ac65df.
13. **Rivera-Salinas, J. E.; Gregorio-Jáuregui, K. M.; Romero-Serrano, J. A.; Cruz-Ramírez, A.; Hernández-Hernández, E.; Miranda-Pérez, A.; Gutierréz-Pérez, V. H.** 2020. Simulation on the Effect of Porosity

in the Elastic Modulus of SiC Particle Reinforced Al Matrix Composites, Metals 10(3): 391. https://doi.org/10.3390/met10030391.
14. **KUPKOVA, M.; PARILAK, L.** 1997. Young's modulus calculations for systems with periodically distributed identical spheroidal pores of various size, orientation, and shape anisotropy, Kovove materialy – Metallic Materials 35(4): 237-246.
15. **Choren, J. A.; Heinrich, S. M.; Silver-Thorn, M. B.** 2013. Young's modulus and volume porosity relationships for additive manufacturing applications, Journal of Materials Science 48: 5103-5112. https://doi.org/10.1007/s10853-013-7237-5.
16. **Chen Z.; Ding F.; Zhang Z.; Liao Q.; Qiao Z.; Jin Y.; Chen M.; Wang B.** 2024. A Review on Machining SiCp/Al Composite Materials, Micromachines 15(1): 107. https://doi.org/10.3390/mi15010107.
17. **Montoya-Dávila M.; Pech-Canul M.I.; Escalera-Lozano R.; Pech-Canul M.A**. 2010. Young's modulus of Al/SiCP/$MgAl_2O_4$ composites with different particle size distribution of reinforcements, Revista Matéria 15(2): 233-239. https://doi.org/10.1590/S1517-70762010000200021.
18. **Dinesh, C. V. S.** 2022. Study on Mechanical, Wear and Thermal Properties ofAL2O3/Graphite Reinforced AA2024 Aluminum Alloy Based Metal Matrix Composites, International Journal for Research in Applied Science and Engineering Technology (IJRASET), 10(12):1390-1403. https://doi.org/10.22214/ijraset.2022.48218.
19. **Dewey, J. M.** 1947. The elastic constants of materials loaded with non-rigid fillers, Journal of Applied Physics 18(6): 578-581. https://doi.org/10.1063/1.1697691.
20. **Paul B.** 1960. Prediction of elastic constants of multiphase materials, Transactions of the Metallurgical Society of AIME 218: 36-41.
21. **Voigt W.** 1889. Über die Beziehung zwischen den beiden Elasticitätsconstanten isotroper Körper, Annalen der Physik (English: Annals of Physics) 38: 573-587. https://doi.org/10.1002/andp.18892741206.
22. **Reuss A.** 1929. Berechnung der Fließgrenze von Mischkristallen auf Grund der Plastizitätsbedingung für Einkristalle, Journal of Applied Mathematics and Mechanics 9: 49-58. https://doi.org/10.1002/zamm.19290090104.
23. **Zhu, S.; Wu, S.; Fu, Y.; and Guo, S.** 2024. Prediction of particle-reinforced composite material properties based on an improved Halpin–Tsai model, AIP Advances 14(4): 045339. https://doi.org/10.1063/5.0206774.
24. **Halpin, J.C.; Tsai, S. W.** 1967. Environmental Factors in Composite Materials Design, Air Force Technical Report AFML-TR: 67-423. Dayton, OH: Wright Aeronautical Laboratories.
25. **Park, H.K.; Jung, J.; Kim, H.S.** 2017. Three-dimensional microstructure modeling of particulate composites using statistical synthetic structure and its thermo-mechanical finite element analysis, Computational Materials Science 126: 265-71. https://doi.org/10.1016/j.commatsci.2016.09.033.
26. **CEA.** (n.d.) Cast3M: Finite element modeling software. Available at: http://www-cast3m.cea.fr/
27. **Laghari, R.A.; Li, J.; Wu, Y.** 2020. Study of Machining Process of SiCp/Al Particle Reinforced Metal Matrix Composite Using Finite Element Analysis and Experimental Verification, Materials 13(23): 5524. https://doi.org/10.3390/ma13235524.
28. **Tohgo, K.; Itoh, Y.; Shimamura, Y.** 2010. A constitutive model of particulate-reinforced composites taking account of particle size effects and damage evolution, Composites Part A: Applied Science and Manufacturing 41(2): 313-21. https://doi.org/10.1016/j.compositesa.2009.10.023.
29. **Mansouri, K.; Chermime, B.; Saoudi, A.; Djebaili, H.; Litim, A.; Kabouche, Z.** 2021. Effect of Reinforcing Particle Shape on the Behavior of Composites Materials, Journal of Nano- and Electronic Physics 13(6): 06018. http://doi.org/10.21272/jnep.13(6).06018.

K. Mansouri, H. Djebaili, F. Khadraoui, M. Chitour, A. Berkia, S. Touati, F. Lekmine, D. Bourmada

SIMULATION ON THE IMPACT OF POROSITY ON THE PROPERTIES OF CERAMIC PARTICLES REINFORCED METAL MATRIX COMPOSITES

S u m m a r y

Although the porosity in Al/SiC metal matrix composites can be reduced, its presence is inevitable. This study aims to investigate the influence of porosity and pore size on the performance of SiC reinforced aluminum matrix composites that contain porosity. To achieve this, we consider both constant and variable diameters of pores, assuming a circular shape while maintaining the same volume fraction. Finite element analysis is conducted on a square matrix reinforced with nine particles subjected to a tensile test. The simulation employs a two-dimensional plane stress model along with square, hexagonal, and random distributions of multiple particles. The results indicate that, despite the presence of pores, the stress transfer from the softer matrix to the reinforcement remains effective. Moreover, the properties of the composite are found to be increasingly sensitive to porosity and pore size, particularly when the pore diameter increases and the distance to the particles decreases.

Keywords: simulation Al/SiC composite, porosity, pore size, finite element analysis.

Received July 15, 2025
Accepted April 24, 2026